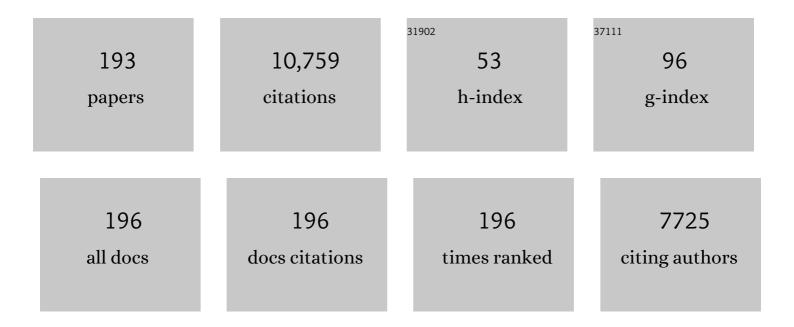
Roger Schibli

List of Publications by Year in descending order

Source: https://exaly.com/author-pdf/3131547/publications.pdf Version: 2024-02-01



#	Article	IF	CITATIONS
1	A Novel Organometallic Aqua Complex of Technetium for the Labeling of Biomolecules:Â Synthesis of [99mTc(OH2)3(CO)3]+from [99mTcO4]-in Aqueous Solution and Its Reaction with a Bifunctional Ligand. Journal of the American Chemical Society, 1998, 120, 7987-7988.	6.6	663
2	Synthesis and Properties of Boranocarbonate:Â A Convenient in Situ CO Source for the Aqueous Preparation of [99mTc(OH2)3(CO)3]+. Journal of the American Chemical Society, 2001, 123, 3135-3136.	6.6	436
3	Metal chelating systems synthesized using the copper(i) catalyzed azide-alkynecycloaddition. Dalton Transactions, 2010, 39, 675-696.	1.6	355
4	Influence of the Denticity of Ligand Systems on the in Vitro and in Vivo Behavior of99mTc(I)â^'Tricarbonyl Complexes:À A Hint for the Future Functionalization of Biomolecules. Bioconjugate Chemistry, 2000, 11, 345-351.	1.8	348
5	Basic aqueous chemistry of [M(OH2)3(CO)3]+ (M=Re, Tc) directed towards radiopharmaceutical application. Coordination Chemistry Reviews, 1999, 190-192, 901-919.	9.5	321
6	Current use and future potential of organometallic radiopharmaceuticals. European Journal of Nuclear Medicine and Molecular Imaging, 2002, 29, 1529-1542.	3.3	295
7	"Click to Chelateâ€ı Synthesis and Installation of Metal Chelates into Biomolecules in a Single Step. Journal of the American Chemical Society, 2006, 128, 15096-15097.	6.6	286
8	Siteâ€Specific and Stoichiometric Modification of Antibodies by Bacterial Transglutaminase. Angewandte Chemie - International Edition, 2010, 49, 9995-9997.	7.2	274
9	First Application offac-[99mTc(OH2)3(CO)3]+in Bioorganometallic Chemistry:Â Design, Structure, and in Vitro Affinity of a 5-HT1AReceptor Ligand Labeled with99mTc. Journal of the American Chemical Society, 1999, 121, 6076-6077.	6.6	231
10	Transglutaminase-Based Chemo-Enzymatic Conjugation Approach Yields Homogeneous Antibody–Drug Conjugates. Bioconjugate Chemistry, 2014, 25, 569-578.	1.8	213
11	Metal carbonyl syntheses XXII. Low pressure carbonylation of [MOCl4]â^' and [MO4]â^': the technetium(I) and rhenium(I) complexes [NEt4]2[MCl3(CO)3]. Journal of Organometallic Chemistry, 1995, 493, 119-127.	0.8	197
12	A Unique Matched Quadruplet of Terbium Radioisotopes for PET and SPECT and for α- and β ^{â^`} -Radionuclide Therapy: An In Vivo Proof-of-Concept Study with a New Receptor-Targeted Folate Derivative. Journal of Nuclear Medicine, 2012, 53, 1951-1959.	2.8	189
13	Steps toward High Specific Activity Labeling of Biomolecules for Therapeutic Application:Â Preparation of Precursor [188Re(H2O)3(CO)3]+and Synthesis of Tailor-Made Bifunctional Ligand Systems. Bioconjugate Chemistry, 2002, 13, 750-756.	1.8	179
14	Folic Acid Conjugates for Nuclear Imaging of Folate Receptor–Positive Cancer. Journal of Nuclear Medicine, 2011, 52, 1-4.	2.8	174
15	"Clickâ€toâ€Chelate†Design and Incorporation of Triazoleâ€Containing Metalâ€Chelating Systems into Biomolecules of Diagnostic and Therapeutic Interest. Chemistry - A European Journal, 2008, 14, 6173-6183.	1.7	165
16	Promising Prospects for ⁴⁴ Sc-/ ⁴⁷ Sc-Based Theragnostics: Application of ⁴⁷ Sc for Radionuclide Tumor Therapy in Mice. Journal of Nuclear Medicine, 2014, 55, 1658-1664.	2.8	163
17	DOTA Conjugate with an Albumin-Binding Entity Enables the First Folic Acid–Targeted ¹⁷⁷ Lu-Radionuclide Tumor Therapy in Mice. Journal of Nuclear Medicine, 2013, 54, 124-131.	2.8	143
18	44Sc-PSMA-617 for radiotheragnostics in tandem with 177Lu-PSMA-617—preclinical investigations in comparison with 68Ga-PSMA-11 and 68Ga-PSMA-617. EINMMI Research, 2017, 7, 9.	1.1	140

#	Article	IF	CITATIONS
19	Reactions with the technetium and rhenium carbonyl complexes (NEt4)2[MX3(CO)3]. Synthesis and structure of [Tc(CN-But)3(CO)3](NO3) and (NEt4)[Tc2(μ-SCH2CH2OH)3(CO)6]. Polyhedron, 1996, 15, 1079-1089.	1.0	135
20	The low-energy βâ^' and electron emitter 161Tb as an alternative to 177Lu for targeted radionuclide therapy. Nuclear Medicine and Biology, 2011, 38, 917-924.	0.3	120
21	Albumin-Binding PSMA Ligands: Optimization of the Tissue Distribution Profile. Molecular Pharmaceutics, 2018, 15, 934-946.	2.3	116
22	Terbium-161 for PSMA-targeted radionuclide therapy of prostate cancer. European Journal of Nuclear Medicine and Molecular Imaging, 2019, 46, 1919-1930.	3.3	109
23	Promises of Cyclotron-Produced ⁴⁴ Sc as a Diagnostic Match for Trivalent β ^ⲳ -Emitters: In Vitro and In Vivo Study of a ⁴⁴ Sc-DOTA-Folate Conjugate. Journal of Nuclear Medicine, 2013, 54, 2168-2174.	2.8	103
24	"Click-to-Chelateâ€! In Vitro and In Vivo Comparison of a ^{99m} Tc(CO) ₃ -Labeled N(ï")-Histidine Folate Derivative with Its Isostructural, Clicked 1,2,3-Triazole Analogue. Bioconjugate Chemistry, 2008, 19, 1689-1695.	1.8	97
25	Preclinical Development of Novel PSMA-Targeting Radioligands: Modulation of Albumin-Binding Properties To Improve Prostate Cancer Therapy. Molecular Pharmaceutics, 2018, 15, 2297-2306.	2.3	97
26	Antibody Conjugates: From Heterogeneous Populations to Defined Reagents. Antibodies, 2015, 4, 197-224.	1.2	96
27	Derivatization of Glucose and 2-Deoxyglucose for Transition Metal Complexation: Substitution Reactions with Organometallic99mTc and Re Precursors and Fundamental NMR Investigations. Chemistry - A European Journal, 2001, 7, 1868-1873.	1.7	94
28	Cyclotron production of 44Sc: From bench to bedside. Nuclear Medicine and Biology, 2015, 42, 745-751.	0.3	91
29	Direct in vitro and in vivo comparison of 161Tb and 177Lu using a tumour-targeting folate conjugate. European Journal of Nuclear Medicine and Molecular Imaging, 2014, 41, 476-485.	3.3	86
30	Hydrolysis of the Organometallic Aqua Ionfac-Triaquatricarbonylrhenium(I). Mechanism, pKa, and Formation Constants of the Polynuclear Hydrolysis Products. Organometallics, 1997, 16, 1833-1840.	1.1	83
31	A "Click Chemistry―Approach to the Efficient Synthesis of Multiple Imaging Probes Derived from a Single Precursor. Bioconjugate Chemistry, 2009, 20, 1940-1949.	1.8	82
32	Synthesis and in Vitro Characterization of Organometallic Rhenium and Technetium Glucose Complexes against Glut 1 and Hexokinase. Bioconjugate Chemistry, 2005, 16, 105-112.	1.8	79
33	¹⁸ Fâ€Radiolabeling of Aromatic Compounds Using Triarylsulfonium Salts. European Journal of Organic Chemistry, 2012, 2012, 889-892.	1.2	77
34	Radioimmunotherapy of Fibroblast Activation Protein Positive Tumors by Rapidly Internalizing Antibodies. Clinical Cancer Research, 2012, 18, 6208-6218.	3.2	74
35	SPECT Study of Folate Receptor-Positive Malignant and Normal Tissues in Mice Using a Novel ^{99m} Tc-Radiofolate. Journal of Nuclear Medicine, 2008, 49, 310-317.	2.8	73
36	Structural and 99Tc NMR Investigations of Complexes with fac-[Tc(CO)3]+ Moieties and Macrocyclic Thioethers of Various Ring Sizes:  Synthesis and X-ray Structure of the Complexes fac-[Tc(9-ane-S3)(CO)3]Br, fac-[Tc2(tosylate)2(18-ane-S6)(CO)6], and fac-[Tc2(20-ane-S6-OH)(CO)6][tosylate]2. Inorganic Chemistry, 1998, 37, 3509-3516.	1.9	72

#	Article	IF	CITATIONS
37	Alpha-PET with terbium-149: evidence and perspectives for radiotheragnostics. EJNMMI Radiopharmacy and Chemistry, 2017, 1, 5.	1.8	72
38	Dosimetry and First Clinical Evaluation of the New ¹⁸ F-Radiolabeled Bombesin Analogue BAY 864367 in Patients with Prostate Cancer. Journal of Nuclear Medicine, 2015, 56, 372-378.	2.8	70
39	Novel Glycated [^{99m} Tc(CO) ₃]-Labeled Bombesin Analogues for Improved Targeting of Gastrin-Releasing Peptide Receptor-Positive Tumors. Bioconjugate Chemistry, 2008, 19, 2432-2439.	1.8	65
40	Folate Receptor Targeted Alpha-Therapy Using Terbium-149. Pharmaceuticals, 2014, 7, 353-365.	1.7	65
41	Preclinical evaluation of novel organometallic 99mTc-folate and 99mTc-pteroate radiotracers for folate receptor-positive tumour targeting. European Journal of Nuclear Medicine and Molecular Imaging, 2006, 33, 1007-1016.	3.3	64
42	Prospects in Folate Receptor-Targeted Radionuclide Therapy. Frontiers in Oncology, 2013, 3, 249.	1.3	63
43	Clinical evaluation of the radiolanthanide terbium-152: first-in-human PET/CT with ¹⁵² Tb-DOTATOC. Dalton Transactions, 2017, 46, 14638-14646.	1.6	61
44	Organometallic 99mTc-technetium(I)- and Re-rhenium(I)-folate derivatives for potential use in nuclear medicine. Journal of Organometallic Chemistry, 2004, 689, 4712-4721.	0.8	60
45	Future prospects for SPECT imaging using the radiolanthanide terbium-155 — production and preclinical evaluation in tumor-bearing mice. Nuclear Medicine and Biology, 2014, 41, e58-e65.	0.3	60
46	47Sc as useful β–-emitter for the radiotheragnostic paradigm: a comparative study of feasible production routes. EJNMMI Radiopharmacy and Chemistry, 2017, 2, 5.	1.8	60
47	Folate Receptor-Positive Gynecological Cancer Cells: In Vitro and In Vivo Characterization. Pharmaceuticals, 2017, 10, 72.	1.7	60
48	Therapeutic Radiometals Beyond ¹⁷⁷ Lu and ⁹⁰ Y: Production and Application of Promising α-Particle, β ^{â^'} -Particle, and Auger Electron Emitters. Journal of Nuclear Medicine, 2017, 58, 91S-96S.	2.8	58
49	Imaging of activated macrophages in experimental osteoarthritis using folate-targeted animal single-photon-emission computed tomography/computed tomography. Arthritis and Rheumatism, 2011, 63, 1898-1907.	6.7	57
50	A Click Approach to Structurally Diverse Conjugates Containing a Central Diâ€1,2,3â€ŧriazole Metal Chelate. ChemMedChem, 2009, 4, 529-539.	1.6	56
51	Production and characterization of no-carrier-added 161Tb as an alternative to the clinically-applied 177Lu for radionuclide therapy. EJNMMI Radiopharmacy and Chemistry, 2019, 4, 12.	1.8	56
52	Tauvid™: The First FDA-Approved PET Tracer for Imaging Tau Pathology in Alzheimer's Disease. Pharmaceuticals, 2021, 14, 110.	1.7	56
53	Complete Carbonylation offac-[Tc(H2O)3(CO)3]+ under CO Pressure in Aqueous Media: A Single Sample Story!. Angewandte Chemie - International Edition, 2000, 39, 254-256.	7.2	54
54	Modification of Different IgG1 Antibodies via Glutamine and Lysine using Bacterial and Human Tissue Transglutaminase. Bioconjugate Chemistry, 2008, 19, 271-278.	1.8	54

#	Article	IF	CITATIONS
55	Quantification of Brain Glucose Metabolism by ¹⁸ F-FDG PET with Real-Time Arterial and Image-Derived Input Function in Mice. Journal of Nuclear Medicine, 2013, 54, 132-138.	2.8	54
56	44Sc for labeling of DOTA- and NODAGA-functionalized peptides: preclinical in vitro and in vivo investigations. EJNMMI Radiopharmacy and Chemistry, 2017, 1, 8.	1.8	53
57	Cholecystokinin 2 Receptor Agonist ¹⁷⁷ Lu-PP-F11N for Radionuclide Therapy of Medullary Thyroid Carcinoma: Results of the Lumed Phase Oa Study. Journal of Nuclear Medicine, 2020, 61, 520-526.	2.8	53
58	Pemetrexed Improves Tumor Selectivity of ¹¹¹ In-DTPA-Folate in Mice with Folate Receptor–Positive Ovarian Cancer. Journal of Nuclear Medicine, 2008, 49, 623-629.	2.8	52
59	First-in-Human PET/CT Imaging of Metastatic Neuroendocrine Neoplasms with Cyclotron-Produced ⁴⁴ Sc-DOTATOC: A Proof-of-Concept Study. Cancer Biotherapy and Radiopharmaceuticals, 2017, 32, 124-132.	0.7	52
60	Towards Translational ImmunoPET/MR Imaging of Invasive Pulmonary Aspergillosis: The Humanised Monoclonal Antibody JF5 Detects <i>Aspergillus</i> Lung Infections <i>In Vivo</i> . Theranostics, 2017, 7, 3398-3414.	4.6	52
61	Development of a new class of PSMA radioligands comprising ibuprofen as an albumin-binding entity. Theranostics, 2020, 10, 1678-1693.	4.6	52
62	Anti-L1CAM radioimmunotherapy is more effective with the radiolanthanide terbium-161 compared to lutetium-177 in an ovarian cancer model. European Journal of Nuclear Medicine and Molecular Imaging, 2014, 41, 1907-1915.	3.3	51
63	Dual, Site‧pecific Modification of Antibodies by Using Solidâ€Phase Immobilized Microbial Transglutaminase. ChemBioChem, 2017, 18, 1923-1927.	1.3	51
64	Evaluation of a novel radiofolate in tumour-bearing mice: promising prospects for folate-based radionuclide therapy. European Journal of Nuclear Medicine and Molecular Imaging, 2009, 36, 938-946.	3.3	49
65	The soluble form of the cancer-associated L1 cell adhesion molecule is a pro-angiogenic factor. International Journal of Biochemistry and Cell Biology, 2009, 41, 1572-1580.	1.2	49
66	Alpha-PET for Prostate Cancer: Preclinical investigation using 149Tb-PSMA-617. Scientific Reports, 2019, 9, 17800.	1.6	49
67	Inhibition of MNK pathways enhances cancer cell response to chemotherapy with temozolomide and targeted radionuclide therapy. Cellular Signalling, 2016, 28, 1412-1421.	1.7	48
68	Synthesis and in Vitro/in Vivo Evaluation of Novel 99mTc(CO)3-Folates. Bioconjugate Chemistry, 2006, 17, 797-806.	1.8	46
69	Isostructural folate conjugates radiolabeled with the matched pair 99mTc/188Re: a potential strategy for diagnosis and therapy of folate receptor-positive tumors. Nuclear Medicine and Biology, 2007, 34, 595-601.	0.3	46
70	Evaluation of ¹¹ C-Me-NB1 as a Potential PET Radioligand for Measuring GluN2B-Containing NMDA Receptors, Drug Occupancy, and Receptor Cross Talk. Journal of Nuclear Medicine, 2018, 59, 698-703.	2.8	46
71	Versatile synthetic approach to new bifunctional chelating agents tailor made for labeling with the fac-[M(CO)3]+ core (M = Tc, 99mTc, Re): synthesis, in vitro, and in vivo behavior of the model complex [M(APPA)(CO)3] (appa = [(5-amino-pentyl)-pyridin-2-yl-methyl-amino]-acetic acid). Nuclear Medicine and Biology. 2003. 30. 465-470.	0.3	44
72	Preclinical Comparison of Albumin-Binding Radiofolates: Impact of Linker Entities on the in Vitro and in Vivo Properties. Molecular Pharmaceutics, 2017, 14, 523-532.	2.3	44

#	Article	IF	CITATIONS
73	Synthesis, In Vitro, and In Silico Evaluation of Organometallic Technetium and Rhenium Thymidine Complexes with Retained Substrate Activity toward Human Thymidine Kinase Type 1. Journal of Medicinal Chemistry, 2008, 51, 6689-6698.	2.9	43
74	Radiosynthesis and Preclinical Evaluation of 3′-Aza-2′-[¹⁸ F]fluorofolic Acid: A Novel PET Radiotracer for Folate Receptor Targeting. Bioconjugate Chemistry, 2013, 24, 205-214.	1.8	43
75	Gene expression levels of matrix metalloproteinases in human atherosclerotic plaques and evaluation of radiolabeled inhibitors as imaging agents for plaque vulnerability. Nuclear Medicine and Biology, 2014, 41, 562-569.	0.3	43
76	Contribution of Auger/conversion electrons to renal side effects after radionuclide therapy: preclinical comparison of 161Tb-folate and 177Lu-folate. EJNMMI Research, 2016, 6, 13.	1.1	43
77	Imaging quality of 44Sc in comparison with five other PET radionuclides using Derenzo phantoms and preclinical PET. Applied Radiation and Isotopes, 2016, 110, 129-133.	0.7	43
78	Tumor targeting using 67Ga-DOTA-Bz-folate — investigations of methods to improve the tissue distribution of radiofolates. Nuclear Medicine and Biology, 2011, 38, 715-723.	0.3	42
79	First-in-Humans Application of ¹⁶¹ Tb: A Feasibility Study Using ¹⁶¹ Tb-DOTATOC. Journal of Nuclear Medicine, 2021, 62, 1391-1397.	2.8	42
80	Regional cerebral blood flow estimated by early PiB uptake is reduced in mild cognitive impairment and associated with age in an amyloid-dependent manner. Neurobiology of Aging, 2015, 36, 1619-1628.	1.5	41
81	⁶⁴ Cu- and ⁶⁸ Ga-Based PET Imaging of Folate Receptor-Positive Tumors: Development and Evaluation of an Albumin-Binding NODAGA–Folate. Molecular Pharmaceutics, 2016, 13, 1979-1987.	2.3	41
82	Preclinical investigations and first-in-human application of 152Tb-PSMA-617 for PET/CT imaging of prostate cancer. EJNMMI Research, 2019, 9, 68.	1.1	39
83	In vitro and in vivo targeting of different folate receptor-positive cancer cell lines with a novel 99mTc-radiofolate tracer. European Journal of Nuclear Medicine and Molecular Imaging, 2006, 33, 1162-1170.	3.3	38
84	Folate receptor-targeted radionuclide therapy: preclinical investigation of anti-tumor effects and potential radionephropathy. Nuclear Medicine and Biology, 2015, 42, 770-779.	0.3	38
85	Evaluation of the Radiolabeled Boronic Acid-Based FAP Inhibitor MIP-1232 for Atherosclerotic Plaque Imaging. Molecules, 2015, 20, 2081-2099.	1.7	37
86	Syntheses and Characterization of Dicarbonylâ^'Nitrosyl Complexes of Technetium(I) and Rhenium(I) in Aqueous Media:Â Spectroscopic, Structural, and DFT Analyses. Inorganic Chemistry, 2005, 44, 683-690.	1.9	36
87	Imaging Atherosclerotic Plaque Inflammation via Folate Receptor Targeting Using a Novel ¹⁸ F-Folate Radiotracer. Molecular Imaging, 2014, 13, 7290.2013.00074.	0.7	35
88	Novel chemoselective ¹⁸ F-radiolabeling of thiol-containing biomolecules under mild aqueous conditions. Chemical Communications, 2016, 52, 6083-6086.	2.2	35
89	Comparative Studies of Substitution Reactions of Rhenium(I) Dicarbonylâ^'Nitrosyl and Tricarbonyl Complexes in Aqueous Media. Inorganic Chemistry, 2005, 44, 6082-6091.	1.9	34
90	Molecular Assembly of Multifunctional ^{99m} Tc Radiopharmaceuticals Using "Clickable― Amino Acid Derivatives. ChemMedChem, 2010, 5, 2026-2038.	1.6	34

#	Article	IF	CITATIONS
91	PEGylation of 99mTc-labeled bombesin analogues improves their pharmacokinetic properties. Nuclear Medicine and Biology, 2011, 38, 997-1009.	0.3	34
92	Preclinical imaging of the co-stimulatory molecules CD80 and CD86 with indium-111-labeled belatacept in atherosclerosis. EJNMMI Research, 2016, 6, 1.	1.1	33
93	Towards non-invasive imaging of vulnerable atherosclerotic plaques by targeting co-stimulatory molecules. International Journal of Cardiology, 2014, 174, 503-515.	0.8	32
94	Combination of terbium-161 with somatostatin receptor antagonists—a potential paradigm shift for the treatment of neuroendocrine neoplasms. European Journal of Nuclear Medicine and Molecular Imaging, 2022, 49, 1113-1126.	3.3	32
95	Functionalization of Glucose at Position C-3 for Transition Metal Coordination:Â Organo-Rhenium Complexes with Carbohydrate Skeletons. Bioconjugate Chemistry, 2005, 16, 421-428.	1.8	31
96	L1â€CAMâ€ŧargeted antibody therapy and ¹⁷⁷ Luâ€radioimmunotherapy of disseminated ovarian cancer. International Journal of Cancer, 2012, 130, 2715-2721.	2.3	31
97	A comparison of three 67/68Ga-labelled exendin-4 derivatives for β-cell imaging on the GLP-1 receptor: the influence of the conjugation site of NODAGA as chelator. EJNMMI Research, 2014, 4, 31.	1.1	31
98	Versatile Routes to C-2- and C-6-Functionalized Glucose Derivatives of Iminodiacetic Acid. Journal of Organic Chemistry, 2003, 68, 512-518.	1.7	30
99	Radiolabeling of rituximab with 188Re and 99mTc using the tricarbonyl technology. Nuclear Medicine and Biology, 2011, 38, 19-28.	0.3	29
100	Effects of the Antifolates Pemetrexed and CB3717 on the Tissue Distribution of 99mTc-EC20 in Xenografted and Syngeneic Tumor-Bearing Mice. Molecular Pharmaceutics, 2010, 7, 597-604.	2.3	28
101	Radioiodinated Folic Acid Conjugates: Evaluation of a Valuable Concept To Improve Tumor-to-Background Contrast. Molecular Pharmaceutics, 2012, 9, 1213-1221.	2.3	28
102	DOTA-Functionalized Polylysine: A High Number of DOTA Chelates Positively Influences the Biodistribution of Enzymatic Conjugated Anti-Tumor Antibody chCE7agl. PLoS ONE, 2013, 8, e60350.	1.1	28
103	Evaluation of 4-oxo-quinoline-based CB2 PET radioligands in R6/2 chorea huntington mouse model and human ALS spinal cord tissue. European Journal of Medicinal Chemistry, 2018, 145, 746-759.	2.6	28
104	Design and Preclinical Evaluation of an Albumin-Binding PSMA Ligand for ⁶⁴ Cu-Based PET Imaging. Molecular Pharmaceutics, 2018, 15, 5556-5564.	2.3	28
105	Synthesis and structures of technetium(I) and rhenium(I) tricarbonyl complexes with bis(diphenylthiophosphoryl)amide, M(CO)3[(Ph2PS)2N](CH3CN) (M = Tc, Re). Polyhedron, 1998, 17, 1303-1309.	1.0	27
106	Preclinical evaluation and test–retest studies of [18F]PSS232, a novel radioligand for targeting metabotropic glutamate receptor 5 (mGlu5). European Journal of Nuclear Medicine and Molecular Imaging, 2015, 42, 128-137.	3.3	27
107	18F-AzaFol for Detection of Folate Receptor-β Positive Macrophages in Experimental Interstitial Lung Disease—A Proof-of-Concept Study. Frontiers in Immunology, 2019, 10, 2724.	2.2	27
108	Longitudinal in vivo evaluation of bone regeneration by combined measurement of multi-pinhole SPECT and micro-CT for tissue engineering. Scientific Reports, 2015, 5, 10238.	1.6	26

#	Article	IF	CITATIONS
109	Cannabinoid receptor type 2 (CB2) as one of the candidate genes in human carotid plaque imaging: Evaluation of the novel radiotracer [11 C]RS-016 targeting CB2 in atherosclerosis. Nuclear Medicine and Biology, 2017, 47, 31-43.	0.3	26
110	Evaluation of the first 44Sc-labeled Affibody molecule for imaging of HER2-expressing tumors. Nuclear Medicine and Biology, 2017, 45, 15-21.	0.3	26
111	Synthesis, characterization and X-ray crystal structure of [Re(L4)(CO)3]Br·2CH3OH (L4=N,N-bis[(2-diphenylphosphino)ethyl]methoxyethylamine): A model compound for novel cationic 99mTc(I)-tricarbonyl radiotracers useful for heart imaging. Inorganica Chimica Acta, 2006, 359, 2479-2488.	1.2	25
112	Charge Dependent Substrate Activity of C3′ and N3 Functionalized, Organometallic Technetium and Rhenium-Labeled Thymidine Derivatives toward Human Thymidine Kinase 1. Bioconjugate Chemistry, 2010, 21, 622-634.	1.8	25
113	Investigation of the chick embryo as a potential alternative to the mouse for evaluation of radiopharmaceuticals. Nuclear Medicine and Biology, 2015, 42, 226-233.	0.3	25
114	Targeted ⁶⁴ Cuâ€labeled gold nanoparticles for dual imaging with positron emission tomography and optical imaging. Journal of Labelled Compounds and Radiopharmaceuticals, 2019, 62, 471-482.	0.5	25
115	Microbial Transglutaminase and câ€mycâ€Tag: A Strong Couple for the Functionalization of Antibodyâ€Like Protein Scaffolds from Discovery Platforms. ChemBioChem, 2015, 16, 861-867.	1.3	24
116	Comparative Studies of Three Pairs of α- and γ-Conjugated Folic Acid Derivatives Labeled with Fluorine-18. Bioconjugate Chemistry, 2016, 27, 74-86.	1.8	24
117	Therapeutic Potential of 47Sc in Comparison to 177Lu and 90Y: Preclinical Investigations. Pharmaceutics, 2019, 11, 424.	2.0	24
118	Effects of antifolate drugs on the cellular uptake of radiofolates in vitro and in vivo. Journal of Nuclear Medicine, 2006, 47, 2057-64.	2.8	24
119	Quantitative positron emission tomography of <scp>mG</scp> luR5 in rat brain with [¹⁸ F]PSS232 at minimal invasiveness and reduced model complexity. Journal of Neurochemistry, 2015, 133, 330-342.	2.1	23
120	The A/T/N model applied through imaging biomarkers in a memory clinic. European Journal of Nuclear Medicine and Molecular Imaging, 2020, 47, 247-255.	3.3	23
121	L1 Cell Adhesion Molecule Confers Radioresistance to Ovarian Cancer and Defines a New Cancer Stem Cell Population. Cancers, 2020, 12, 217.	1.7	23
122	Radiation dosimetry of 18F-AzaFol: A first in-human use of a folate receptor PET tracer. EJNMMI Research, 2020, 10, 32.	1.1	23
123	Dose-dependent effects of (anti)folate preinjection on 99mTc-radiofolate uptake in tumors and kidneys. Nuclear Medicine and Biology, 2007, 34, 603-608.	0.3	22
124	Single Photon Emission Computed Tomography Tracer. Recent Results in Cancer Research, 2013, 187, 65-105.	1.8	20
125	Synthesis and Biological Evaluation of Thiophene-Based Cannabinoid Receptor Type 2 Radiotracers for PET Imaging. Frontiers in Neuroscience, 2016, 10, 350.	1.4	20
126	Triazolo-Peptidomimetics: Novel Radiolabeled Minigastrin Analogs for Improved Tumor Targeting. Journal of Medicinal Chemistry, 2020, 63, 4484-4495.	2.9	20

#	Article	IF	CITATIONS
127	Design of Radiolabeled Analogs of Minigastrin by Multiple Amide-to-Triazole Substitutions. Journal of Medicinal Chemistry, 2020, 63, 4496-4505.	2.9	20
128	Evaluation of ¹¹¹In-Labelled Exendin-4 Derivatives Containing Different Meprin β-Specific Cleavable Linkers. PLoS ONE, 2015, 10, e0123443.	1.1	20
129	CD80 Is Upregulated in a Mouse Model with Shear Stress-Induced Atherosclerosis and Allows for Evaluating CD80-Targeting PET Tracers. Molecular Imaging and Biology, 2017, 19, 90-99.	1.3	19
130	Evaluation of Actinium-225 Labeled Minigastrin Analogue [225Ac]Ac-DOTA-PP-F11N for Targeted Alpha Particle Therapy. Pharmaceutics, 2020, 12, 1088.	2.0	19
131	Imaging atherosclerotic plaque inflammation via folate receptor targeting using a novel 18F-folate radiotracer. Molecular Imaging, 2014, 13, 1-11.	0.7	19
132	Synthesis and Preliminary Evaluation of a 2-Oxoquinoline Carboxylic Acid Derivative for PET Imaging the Cannabinoid Type 2 Receptor. Pharmaceuticals, 2014, 7, 339-352.	1.7	17
133	Simultaneous Visualization of 161Tb- and 177Lu-Labeled Somatostatin Analogues Using Dual-Isotope SPECT Imaging. Pharmaceutics, 2021, 13, 536.	2.0	17
134	PEGylation, increasing specific activity and multiple dosing as strategies to improve the risk-benefit profile of targeted radionuclide therapy with 177Lu-DOTA-bombesin analogues. EJNMMI Research, 2012, 2, 24.	1.1	16
135	GABAA receptor subtypes in the mouse brain: Regional mapping and diazepam receptor occupancy by in vivo [18F]flumazenil PET. NeuroImage, 2017, 150, 279-291.	2.1	16
136	A first-in-man PET study of [18F]PSS232, a fluorinated ABP688 derivative for imaging metabotropic glutamate receptor subtype 5. European Journal of Nuclear Medicine and Molecular Imaging, 2018, 45, 1041-1051.	3.3	16
137	Promising potential of [177Lu]Lu-DOTA-folate to enhance tumor response to immunotherapy—a preclinical study using a syngeneic breast cancer model. European Journal of Nuclear Medicine and Molecular Imaging, 2021, 48, 984-994.	3.3	16
138	Evaluation of a Novel Tc-99m Labelled Vitamin B12 Derivative for Targeting Escherichia coli and Staphylococcus aureus In Vitro and in an Experimental Foreign-Body Infection Model. Molecular Imaging and Biology, 2015, 17, 829-837.	1.3	15
139	Pharmacological inhibition of mTORC1 increases CCKBR-specific tumor uptake of radiolabeled minigastrin analogue [¹⁷⁷ Lu]Lu-PP-F11N. Theranostics, 2020, 10, 10861-10873.	4.6	15
140	Implementation of a new separation method to produce qualitatively improved <scp>⁶⁴Cu</scp> . Journal of Labelled Compounds and Radiopharmaceuticals, 2019, 62, 460-470.	0.5	14
141	165Er: A new candidate for Auger electron therapy and its possible cyclotron production from natural holmium targets. Applied Radiation and Isotopes, 2020, 159, 109079.	0.7	14
142	Enzymatic Antibody Modification by Bacterial Transglutaminase. Methods in Molecular Biology, 2013, 1045, 205-215.	0.4	13
143	Paclitaxel improved anti-L1CAM lutetium-177 radioimmunotherapy in an ovarian cancer xenograft model. EJNMMI Research, 2014, 4, 54.	1.1	13
144	Chemoselective ¹⁸ F-incorporation into pyridyl acyltrifluoroborates for rapid radiolabelling of peptides and proteins at room temperature. Chemical Communications, 2020, 56, 723-726.	2.2	13

#	Article	IF	CITATIONS
145	1,5-Disubstituted 1,2,3-Triazoles as Amide Bond Isosteres Yield Novel Tumor-Targeting Minigastrin Analogs. ACS Medicinal Chemistry Letters, 2021, 12, 585-592.	1.3	13
146	Elucidating the Structure–Activity Relationship of the Pentaglutamic Acid Sequence of Minigastrin with Cholecystokinin Receptor Subtype 2. Bioconjugate Chemistry, 2019, 30, 657-666.	1.8	12
147	Albumin-Binding PSMA Radioligands: Impact of Minimal Structural Changes on the Tissue Distribution Profile. Molecules, 2020, 25, 2542.	1.7	12
148	In Vivo Imaging of Local Inflammation: Monitoring LPS-Induced CD80/CD86 Upregulation by PET. Molecular Imaging and Biology, 2021, 23, 196-207.	1.3	12
149	Radiosynthesis and evaluation of an 18F–labeled silicon containing exendin-4 peptide as a PET probe for imaging insulinoma. EJNMMI Radiopharmacy and Chemistry, 2018, 3, 1.	1.8	11
150	Production of Mass-Separated Erbium-169 Towards the First Preclinical in vitro Investigations. Frontiers in Medicine, 2021, 8, 643175.	1.2	11
151	In vivo Imaging of Cannabinoid Type 2 Receptors: Functional and Structural Alterations in Mouse Model of Cerebral Ischemia by PET and MRI. Molecular Imaging and Biology, 2022, 24, 700-709.	1.3	11
152	FDG kinetic modeling in small rodent brain PET: optimization of data acquisition and analysis. EJNMMI Research, 2013, 3, 61.	1.1	10
153	A Short-Term Biological Indicator for Long-Term Kidney Damage after Radionuclide Therapy in Mice. Pharmaceuticals, 2017, 10, 57.	1.7	10
154	Reduced 18F-Folate Conjugates as a New Class of PET Tracers for Folate Receptor Imaging. Bioconjugate Chemistry, 2018, 29, 1119-1130.	1.8	10
155	Combination of lutetium-177 labelled anti-L1CAM antibody chCE7 with the clinically relevant protein kinase inhibitor MK1775: a novel combination against human ovarian carcinoma. BMC Cancer, 2018, 18, 922.	1.1	10
156	Preclinical evaluation of 5-methyltetrahydrofolate-based radioconjugates—new perspectives for folate receptor–targeted radionuclide therapy. European Journal of Nuclear Medicine and Molecular Imaging, 2021, 48, 972-983.	3.3	10
157	Impact of the mouse model and molar amount of injected ligand on the tissue distribution profile of PSMA radioligands. European Journal of Nuclear Medicine and Molecular Imaging, 2022, 49, 470-480.	3.3	10
158	Single Photon Emission Computed Tomography Tracer. Recent Results in Cancer Research, 2020, 216, 227-282.	1.8	10
159	Can Nuclear Imaging of Activated Macrophages with Folic Acid-Based Radiotracers Serve as a Prognostic Means to Identify COVID-19 Patients at Risk?. Pharmaceuticals, 2020, 13, 238.	1.7	9
160	Preclinical investigations using [177Lu]Lu-Ibu-DAB-PSMA toward its clinical translation for radioligand therapy of prostate cancer. European Journal of Nuclear Medicine and Molecular Imaging, 2022, 49, 3639-3650.	3.3	9
161	Combining Albumin-Binding Properties and Interaction with Pemetrexed to Improve the Tissue Distribution of Radiofolates. Molecules, 2018, 23, 1465.	1.7	8
162	Diastereomerically Pure 6 <i>R</i> - and 6 <i>S</i> -3′-Aza-2′- ¹⁸ F-Fluoro-5-Methyltetrahydrofolates Show Unprecedentedly High Uptake in Folate Receptor–Positive KB Tumors. Journal of Nuclear Medicine, 2019, 60, 135-141.	2.8	8

#	Article	IF	CITATIONS
163	Identification of a PET Radiotracer for Imaging of the Folate Receptor-α: A Potential Tool to Select Patients for Targeted Tumor Therapy. Journal of Nuclear Medicine, 2021, 62, 1475-1481.	2.8	8
164	Improved Tumor-Targeting with Peptidomimetic Analogs of Minigastrin 177Lu-PP-F11N. Cancers, 2021, 13, 2629.	1.7	8
165	Water-Exchange Study Revealed Unexpected Substitution Behavior of [(CO)2(NO)Re(H2O)3]2+in Aqueous Media. Inorganic Chemistry, 2006, 45, 4199-4204.	1.9	7
166	Synthesis and Evaluation of Novel α-Fluorinated (<i>E</i>)-3-((6-Methylpyridin-2-yl)ethynyl)cyclohex-2-enone- <i>O</i> -methyl Oxime (ABP688) Derivatives as Metabotropic Glutamate Receptor Subtype 5 PET Radiotracers. Journal of Medicinal Chemistry, 2012, 55, 7154-7162.	2.9	7
167	Physiologically Based Pharmacokinetic Modelling with Dynamic PET Data to Study the <i> In Vivo</i> Effects of Transporter Inhibition on Hepatobiliary Clearance in Mice. Contrast Media and Molecular Imaging, 2018, 2018, 1-11.	0.4	7
168	Synthesis and Structure–Affinity Relationship of Small Molecules for Imaging Human CD80 by Positron Emission Tomography. Journal of Medicinal Chemistry, 2019, 62, 8090-8100.	2.9	7
169	Recent progress in allosteric modulators for GluN2A subunit and development of GluN2Aâ€selective nuclear imaging probes. Journal of Labelled Compounds and Radiopharmaceuticals, 2019, 62, 552-560.	0.5	7
170	[11C]mHED PET follows a two-tissue compartment model in mouse myocardium with norepinephrine transporter (NET)-dependent uptake, while [18F]LMI1195 uptake is NET-independent. EJNMMI Research, 2020, 10, 114.	1.1	7
171	Development of High Brain-Penetrant and Reversible Monoacylglycerol Lipase PET Tracers for Neuroimaging. Journal of Medicinal Chemistry, 2022, 65, 2191-2207.	2.9	7
172	Design and Evaluation of Novel Albumin-Binding Folate Radioconjugates: Systematic Approach of Varying the Linker Entities. Molecular Pharmaceutics, 2022, 19, 963-973.	2.3	7
173	Preclinical Investigations to Explore the Difference between the Diastereomers [¹⁷⁷ Lu]Lu-SibuDAB and [¹⁷⁷ Lu]Lu-RibuDAB toward Prostate Cancer Therapy. Molecular Pharmaceutics, 2022, 19, 2105-2114.	2.3	7
174	[¹⁸ F]Flurpiridaz: Facile and Improved Precursor Synthesis for this Nextâ€Generation Cardiac Positron Emission Tomography Imaging Agent. ChemMedChem, 2020, 15, 1040-1043.	1.6	6
175	Role of sex hormones in modulating myocardial perfusion and coronary flow reserve. European Journal of Nuclear Medicine and Molecular Imaging, 2022, 49, 2209-2218.	3.3	6
176	Discovery, synthesis and evaluation of novel reversible monoacylglycerol lipase radioligands bearing a morpholine-3-one scaffold. Nuclear Medicine and Biology, 2022, 108-109, 24-32.	0.3	6
177	Distance-Dependent Cellular Uptake of Oligoproline-Based Homobivalent Ligands Targeting GPCRs—An Experimental and Computational Analysis. Bioconjugate Chemistry, 2020, 31, 2431-2438.	1.8	5
178	Neuroimaging with Radiopharmaceuticals Targeting the Glutamatergic System. Chimia, 2020, 74, 960-967.	0.3	5
179	Targeted Radiotherapeutics from 'Bench-to-Bedside'. Chimia, 2022, 74, 939.	0.3	5
180	Exploring the signaling space of a GPCR using bivalent ligands with a rigid oligoproline backbone. Proceedings of the National Academy of Sciences of the United States of America, 2021, 118, .	3.3	5

#	Article	IF	CITATIONS
181	Ketamine and Ceftriaxone-Induced Alterations in Glutamate Levels Do Not Impact the Specific Binding of Metabotropic Glutamate Receptor Subtype 5 Radioligand [18F]PSS232 in the Rat Brain. Pharmaceuticals, 2018, 11, 83.	1.7	4
182	Combination of Proton Therapy and Radionuclide Therapy in Mice: Preclinical Pilot Study at the Paul Scherrer Institute. Pharmaceutics, 2019, 11, 450.	2.0	4
183	Therapeutic Response of CCKBR-Positive Tumors to Combinatory Treatment with Everolimus and the Radiolabeled Minigastrin Analogue [177Lu]Lu-PP-F11N. Pharmaceutics, 2021, 13, 2156.	2.0	4
184	Rest/stress myocardial perfusion imaging by positron emission tomography with 18F-Flurpiridaz: A feasibility study in mice. Journal of Nuclear Cardiology, 2023, 30, 62-73.	1.4	4
185	Folate Receptor-Targeted Radionuclide Imaging Agents. , 2011, , 65-92.		3
186	Synthesis and in vitro/in vivo pharmacological evaluation of [11C]-ThioABP, a novel radiotracer for imaging mGluR5 with PET. MedChemComm, 2013, 4, 520.	3.5	3
187	Synthesis and Biological Evaluation of Quinoxaline Derivatives for <scp>PET</scp> Imaging of the <scp>NMDA</scp> Receptor. Helvetica Chimica Acta, 2017, 100, e1700204.	1.0	3
188	Unexpected reactivity of cyclic perfluorinated iodanes with electrophiles. Chemical Communications, 2018, 54, 8999-9002.	2.2	3
189	Novel Synthetic Strategies Enable the Efficient Development of Folate Conjugates for Cancer Radiotheranostics. Bioconjugate Chemistry, 2021, 32, 1617-1628.	1.8	3
190	Radiation dosimetry of [18F]-PSS232—a PET radioligand for imaging mGlu5 receptors in humans. EJNMMI Research, 2019, 9, 56.	1.1	2
191	Evaluation of 5 H â€Thiazolo[3,2â€Î±]pyrimidinâ€5â€ones as Potential GluN2A PET Tracers. ChemMedChem, 202 15, 2448-2461.	20 _{1.6}	2
192	Improved Syntheses of the mGlu5 Antagonists MMPEP and MTEP Using Sonogashira Cross-Coupling. Pharmaceuticals, 2018, 11, 24.	1.7	0
193	Terbium radionuclides for theranostics. , 2021, , .		0